Mechanism Aspects of the Hydrogenation of Acrylonitrile on Ni and Pd Surfaces

Xin Ge [ab], Jiongbin Pan [a], Xinzhi Chen [a], Chao Qian [a]* and Shaodong Zhou [c]*

[a] *Key Laboratory of Biomass Chemical Engineering of Ministry of Education, College of Chemical and Biological Engineering, Zhejiang University, Hangzhou, P.R China.*

[b] *School of Chemical and Material Engineering, Jiangnan University, Wuxi, P.R China*

[c] *Institut für Chemie, Technische Universität Berlin, Berlin, Germany*

Outline

* Corresponding author. Chao Qian, E-mail: qianchao@zju.edu.cn and Shaodong Zhou, E-mail: shaodong.zhou@campus.tu-berlin.de

Experimental

GC analyses were performed on GC Agilent 1790F series, and GC-MS analyses were performed on GC-MS Agilent 5973-6890 series. Raney Ni and Raney Cu were purchased from Zhejiang Metallurgical Research Institute Co., Ltd. The apparent density of Raney Ni is about 3.0 g/cm^3 and a mean particle size is about 16.58 μm. All reagents and solvents were general reagent grade. All reactions were carried out in a 250 ml autoclave (Parr 4576 series), which is connected to a computer conjugated detector.

Catalytic hydrogenation of acrylonitrile

The hydrogenation of acrylonitrile was conducted in a 250 ml autoclave Parr 4576 series with mechanical stirring, and the stirring speed, temperature and pressure were monitored and controlled online, as shown in Fig.1. The autoclave was purged with nitrogen for three times and then with hydrogen for another three times, then filled with hydrogen of 2.0 MPa at room temperature. The hydrogen pressure in the hydrogen reservoir (2 L) was maintained at 5.0 MPa, then the inflow valve **2** was shut up. Subsequently, the mixture was heated to 363 K and the pressure increased to 2.2 MPa. Next, the stirring was started and the connection valve **8** was opened and controlled to adjust pressure in the autoclave. Via a pressure sensor that is adapted for online communication, the reaction was monitored with a remote computer. When the cumulative hydrogen absorption capacity achieved the theoretical value or the slope of the hydrogen absorption curve was greatly degraded, the reaction and the date collection was over. The experiment data of hydrogen pressure and reaction time was auto-recorded by computer. Raney Ni was recovered by filtration and washed by methanol. The final product was analyzed by GC or GC-MS.

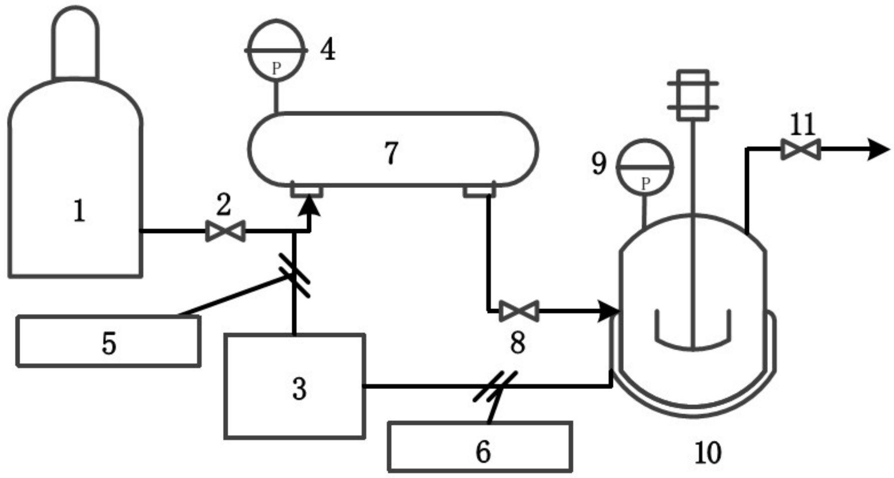

Fig.S1 Experimental device of acrylohydrogenation of nitrile

1-Hydrogen source; 2,8,11-valve; 3-computer; 4,9-hydrogen pressure gauge; 5-pressure sensor; 6-temperature sensor; 7- hydrogen reservoir; 10-autocalve

Fig.S2 MS spectrum of propylamine

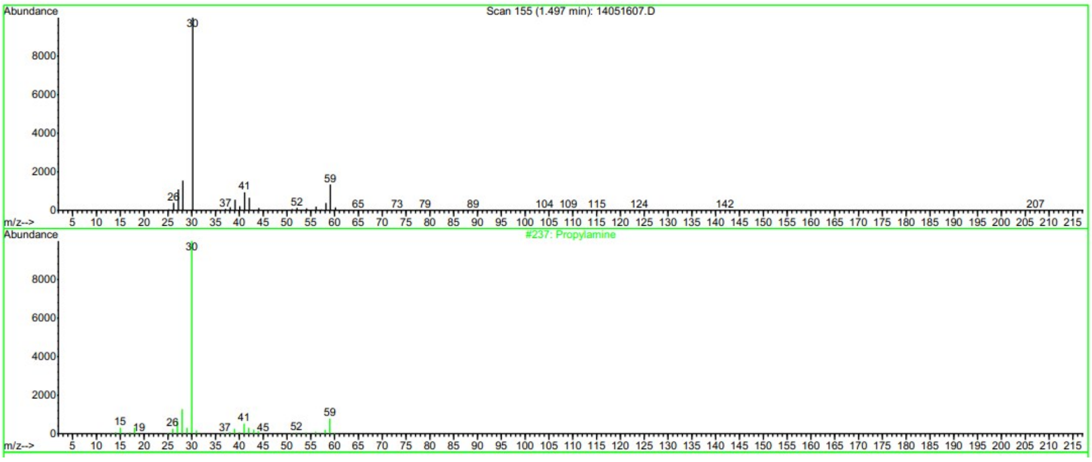

MS (EI, 70eV), *m/z* (rel abundance) : 30(M^+, 100), 59(13), 41(9).

Fig.S3 MS spectrum of dipropylamine

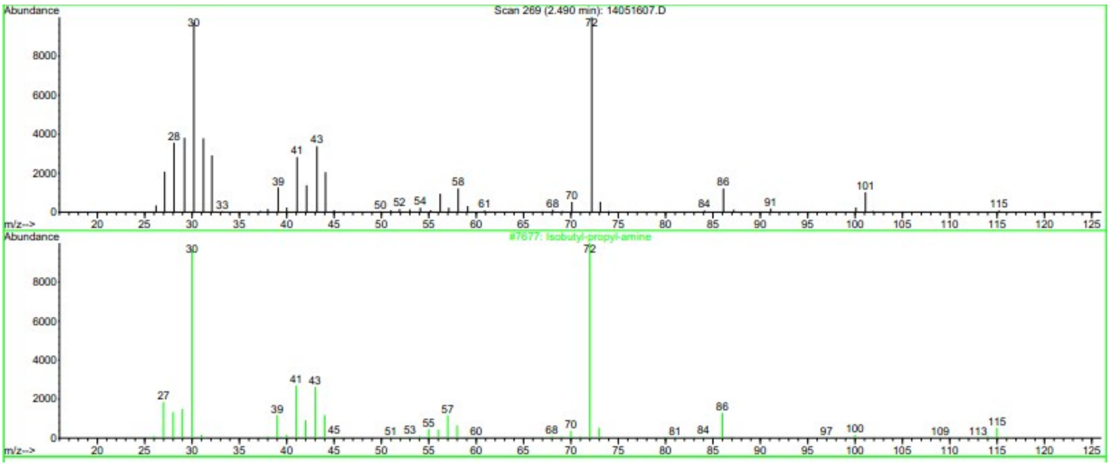

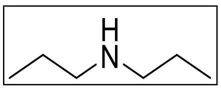

MS (EI, 70eV), *m/z* (rel abundance) : 72(M^+, 100), 30(98), 28(37), 43(35), 86(12), 58(12).

Fig.S4 MS spectrum of 3-(propylamino)propanenitrile

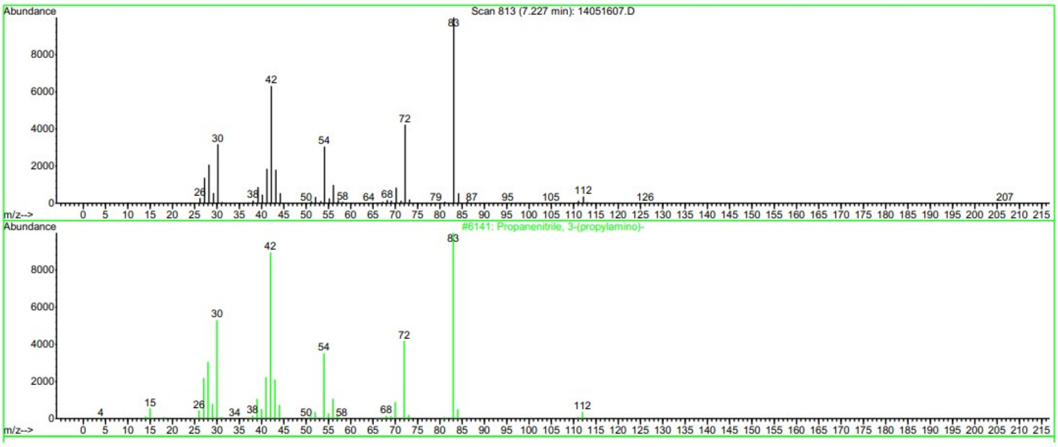

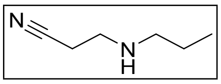

MS (EI, 70eV), *m/z* (rel abundance) : 83(M$^+$, 100), 112(4), 72(43), 54(29), 42(64), 30(32).

Fig.S5 MS spectrum of 3-(dipropylamino)propanenitrile

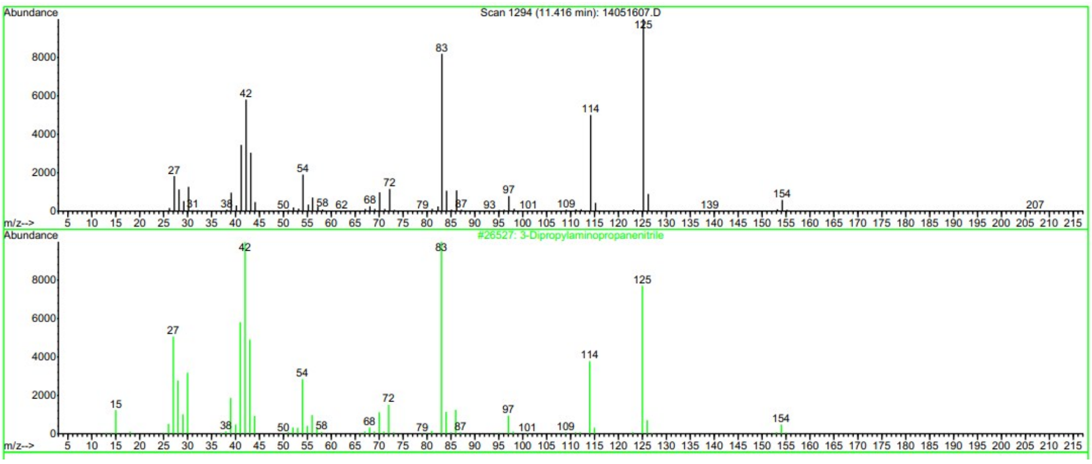

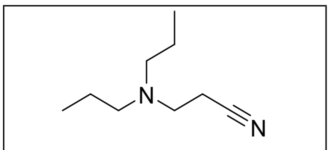

3-(dipropylamino)propanenitrile

MS (EI, 70eV), *m/z* (rel abundance) : 125(M$^+$, 100), 154(4), 114(51), 83(76), 42(60), 54(20), 27(17).

Fig.S6 The adsorption site, energies (in kJ/mol) structural parameters of acrylonitrile adsorbed on Ni(111) and Pd(111)

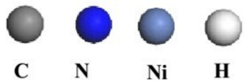

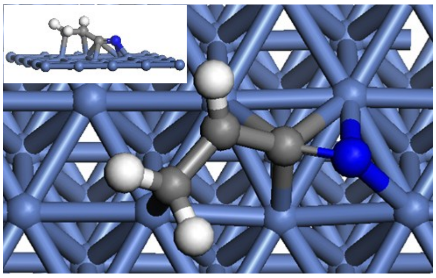

N-fcc-C3-hcp

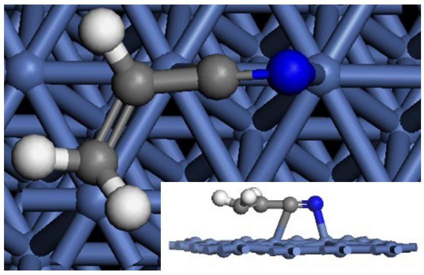

bridge

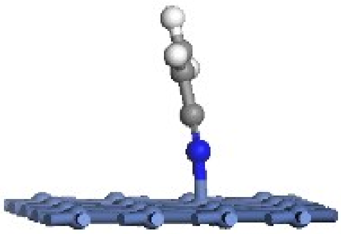

Top

bond	Bond lengths(Å)			
	AN	AN-Ni(111)(N-fcc-C3-hcp)	AN-Ni(111)(bridge)	AN-Ni(111)(top)
C1-C2	1.344	1.466	1.481	1.347
C2-C3	1.427	1.451	1.400	1.398
C3-N	1.183	1.300	1.223	1.180
C1-Ni		1.981		
C2-Ni		2.029		
C3-Ni		2.135, 1.875	2.105	
N-Ni		1.940, 2.004	1.941	1.792

Sites	E_{ad}
N-fcc-C3-fcc	-154.8
bridge	-141.3
Top	-119.2

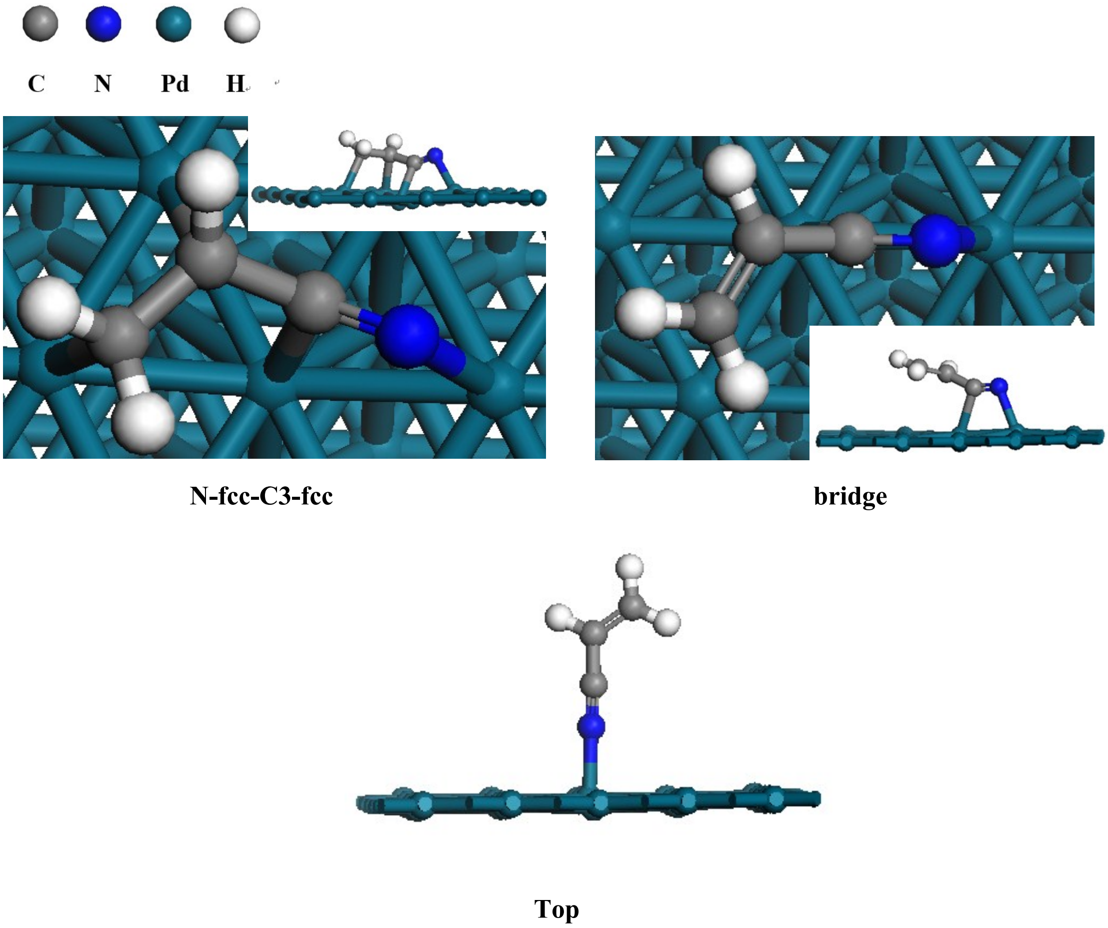

bond	Bond lengths(Å)			
	AN	AN-Pd(111)(N-fcc-C3-fcc)	AN-Pd(111)(bridge)	AN-Pd(111)(top)
C1-C2	1.344	1.459	1.353	1.345
C2-C3	1.427	1.463	1.447	1.409
C3-N	1.183	1.248	1.228	1.179
C1-Pd		2.146		

C2-Pd	2.167		
C3-Pd	2.141	2.135	
N-Pd	2.095	2.084	2.021

Sites	$\boldsymbol{E}_{\mathbf{ad}}$
N-fcc-C3-fcc	-148.12
bridge	-126.53
Top	-120.9

Fig.S7 Energy profile of acrylonitrile hydrogenation to propionitrile on Ni(111)

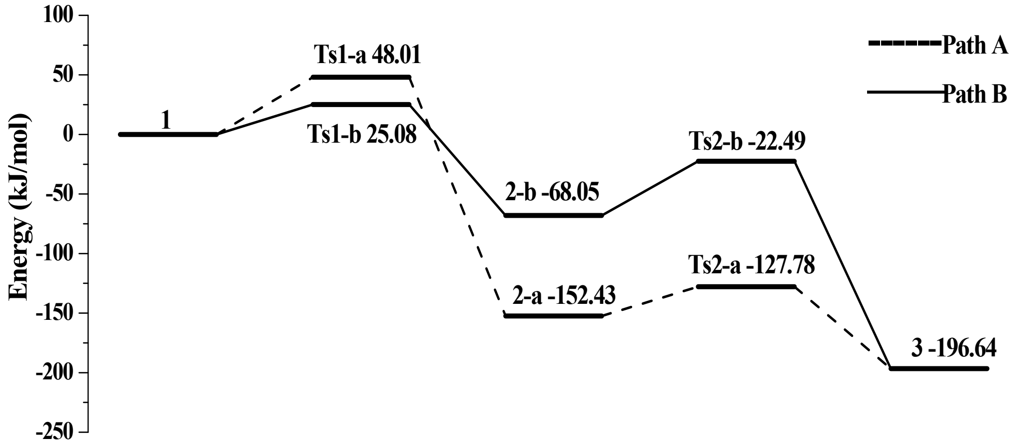

1	Ts1-a	2-a	Ts2-a
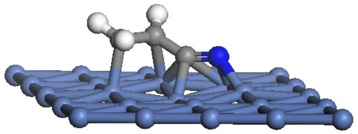	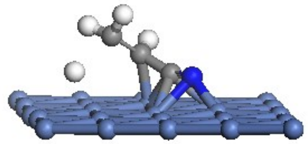	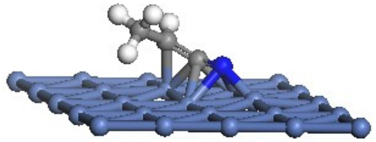	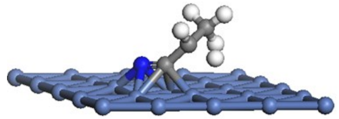
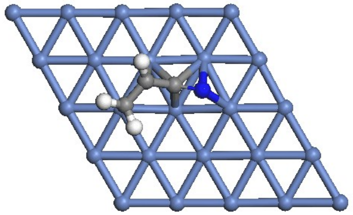	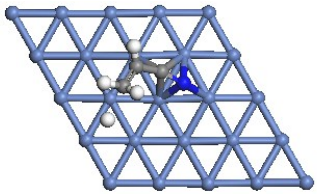	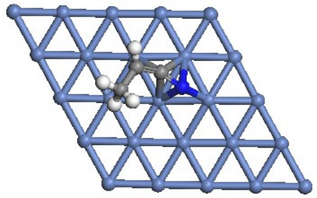	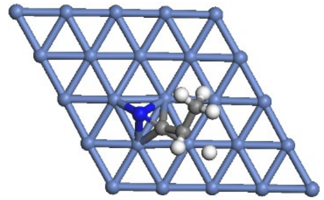
Ts1-b	**2-b**	**Ts2-b**	**3**
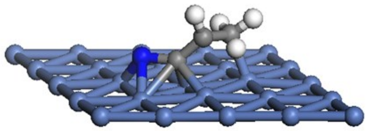	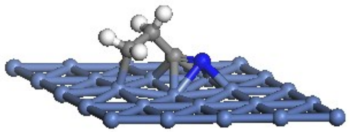	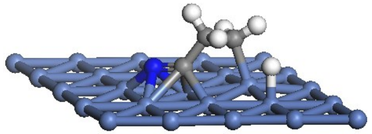	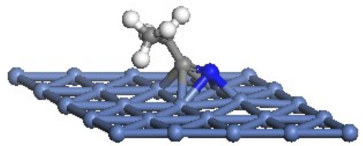
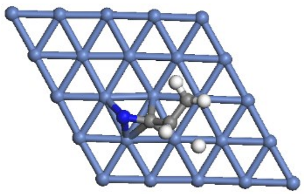	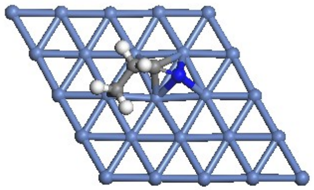	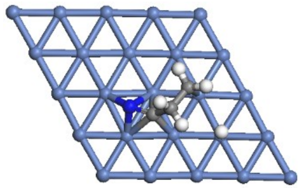	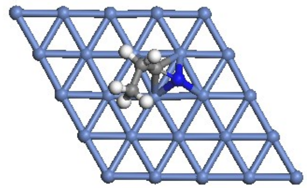

Fig.S8 Energy profile of acrylonitrile hydrogenation to propionitrile on Pd(111)

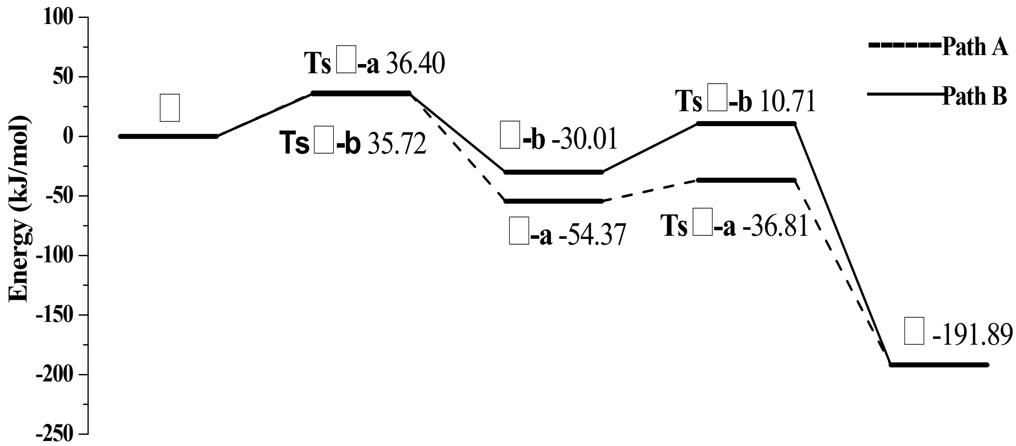

①	Ts①-a	②-a	Ts ②-a
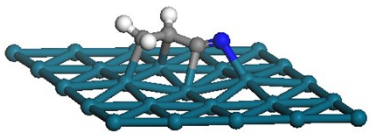	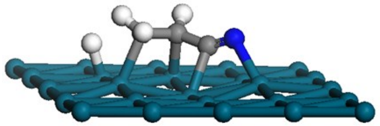	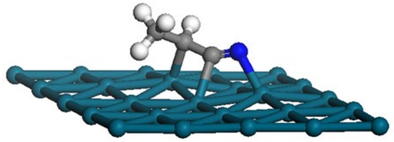	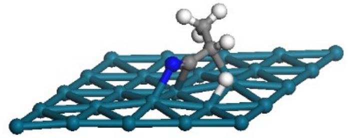
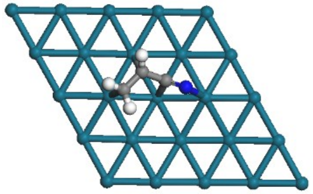	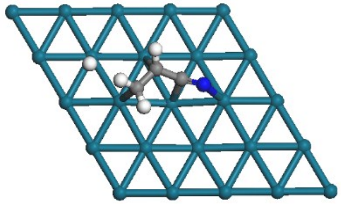	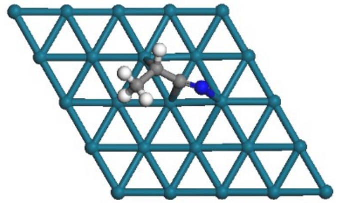	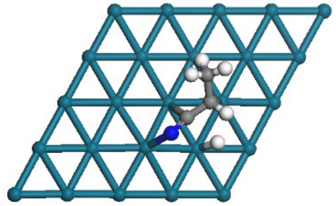
Ts①-b	**②-b**	**Ts②-b**	**③**
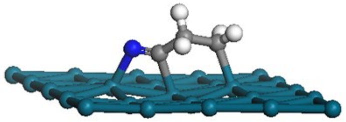	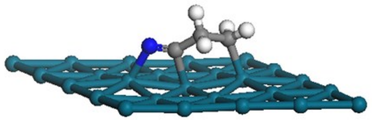	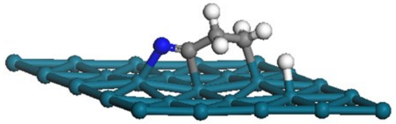	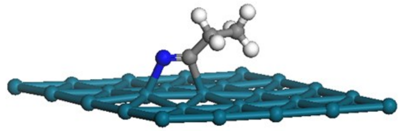
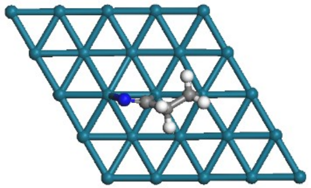	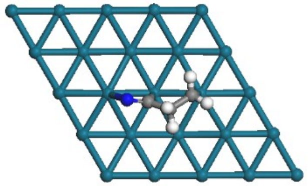	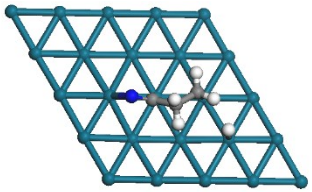	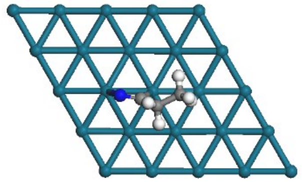

Fig.S9 Energy profile of imine formation on Ni(111)

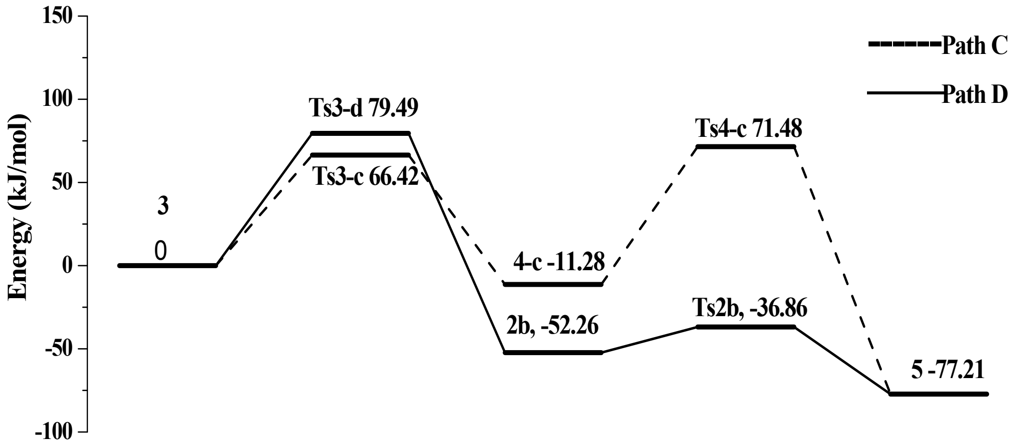

3	Ts3-c	4-c	Ts4-c
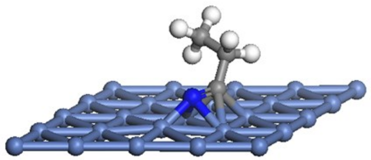	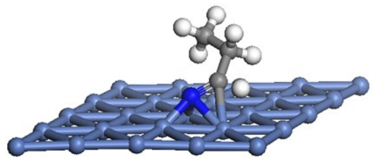	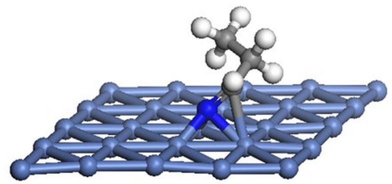	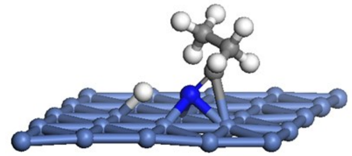
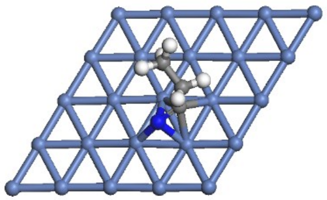	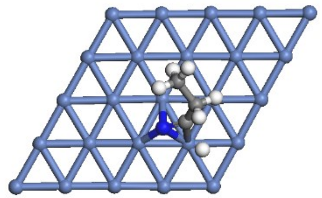	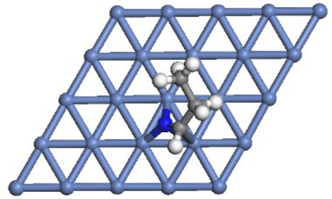	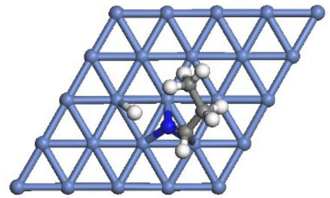
Ts3-d	**4-d**	**Ts4-d**	**5**
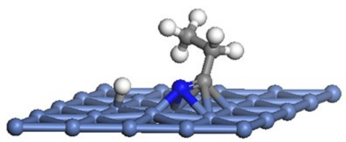	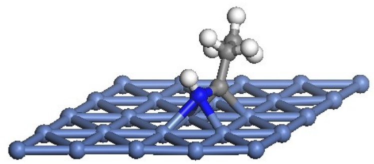	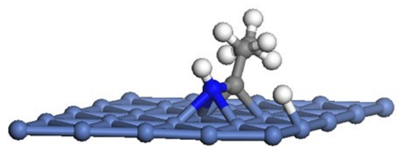	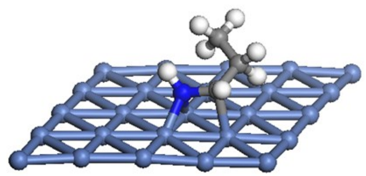
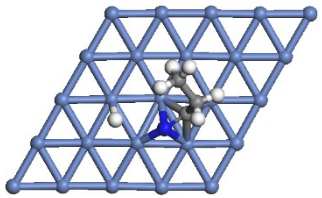	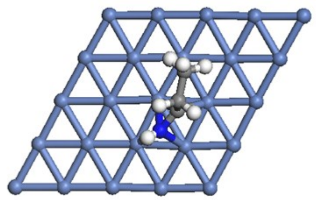	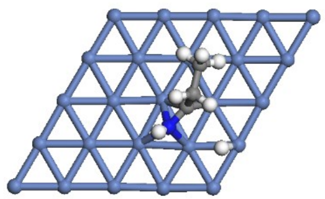	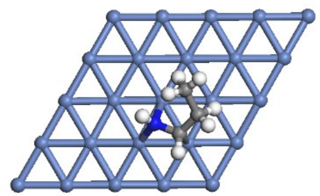

Fig.S10 Energy profile of imine formation on Pd(111)

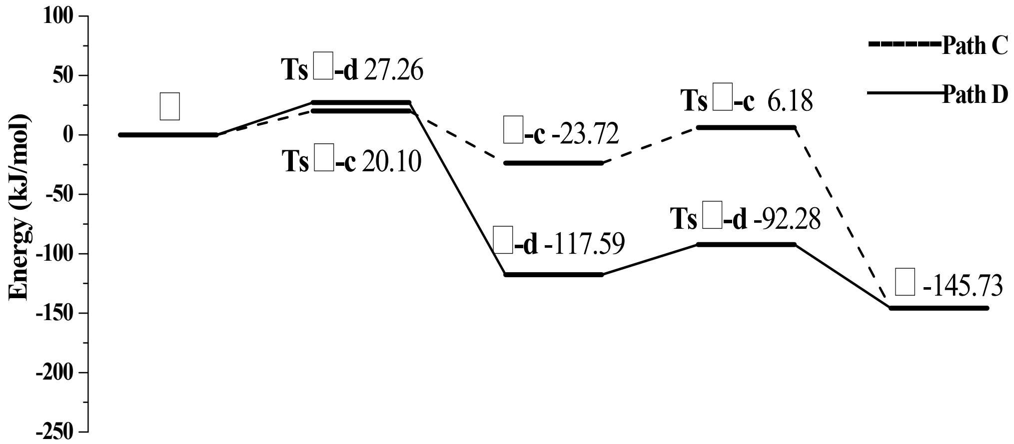

③	Ts ③-c	④-c	Ts ④-c
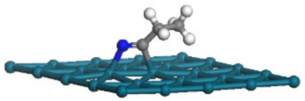	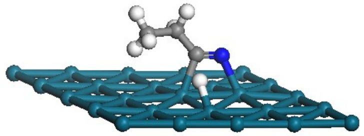	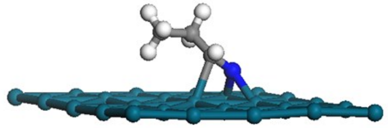	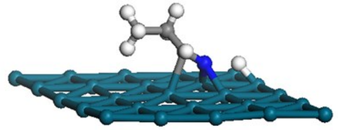
	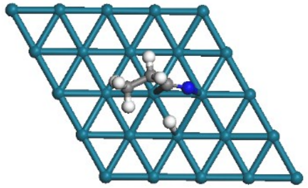	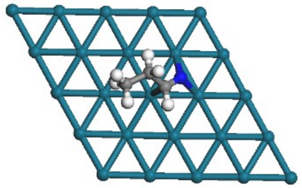	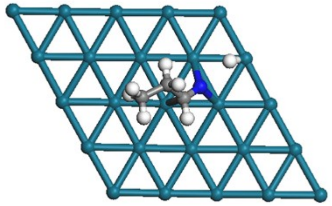
Ts ③-d	**④-d**	**Ts ④-d**	⑤
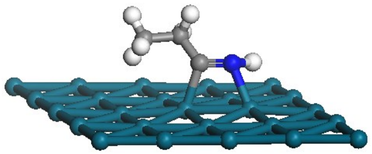	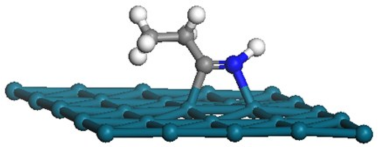	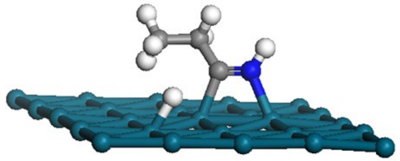	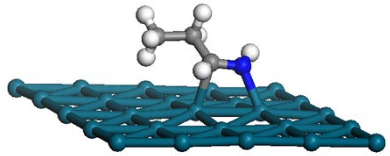
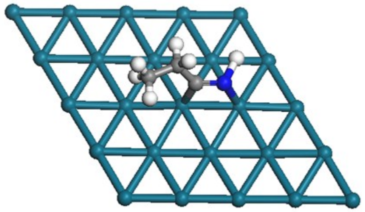	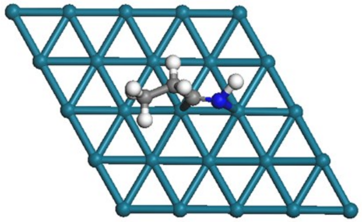	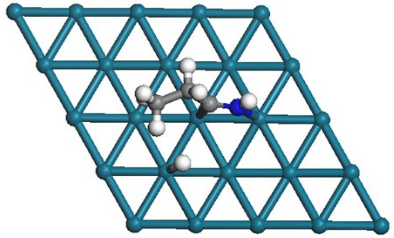	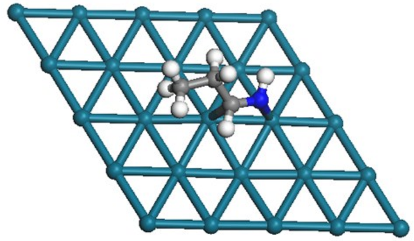

Fig.S11 Energy profile of propylamine formation on Ni(111)

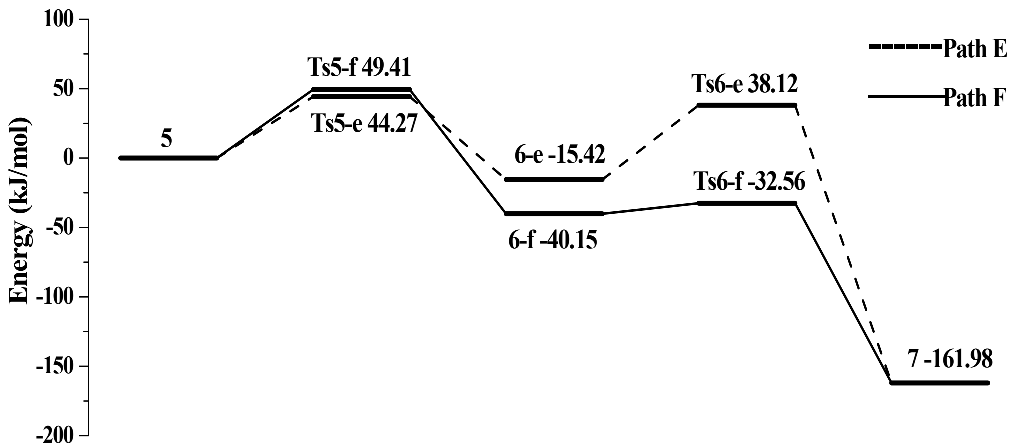

5	Ts5-e	6-e	Ts6-e
	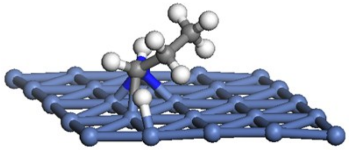	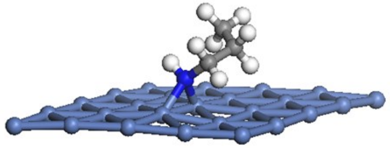	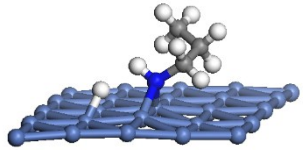
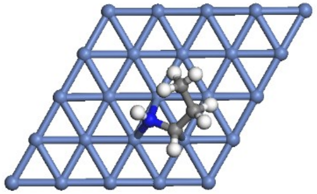	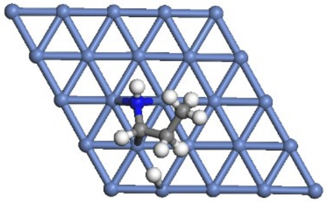	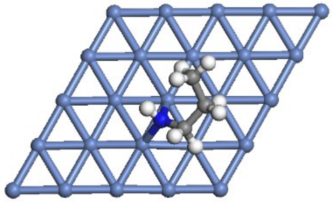	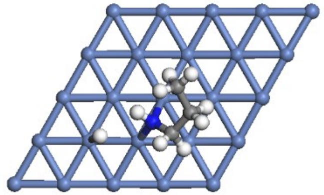
Ts5-f	**6-f**	**Ts6-f**	**7**
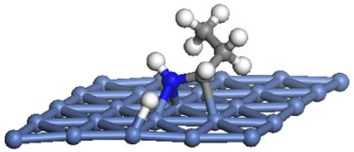	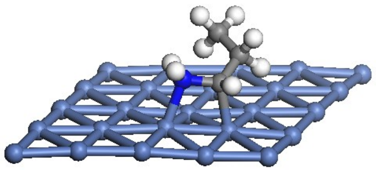	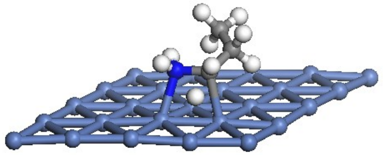	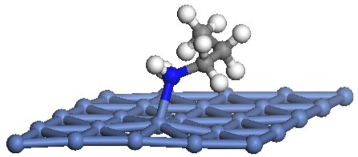
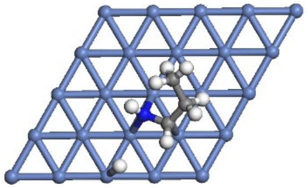	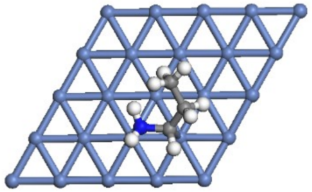	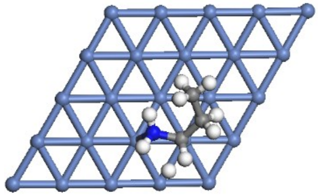	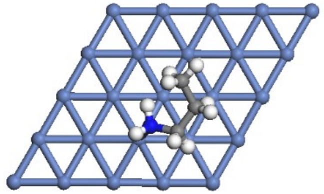

Fig.S12 Energy profile of propylamine formation on Pd(111)

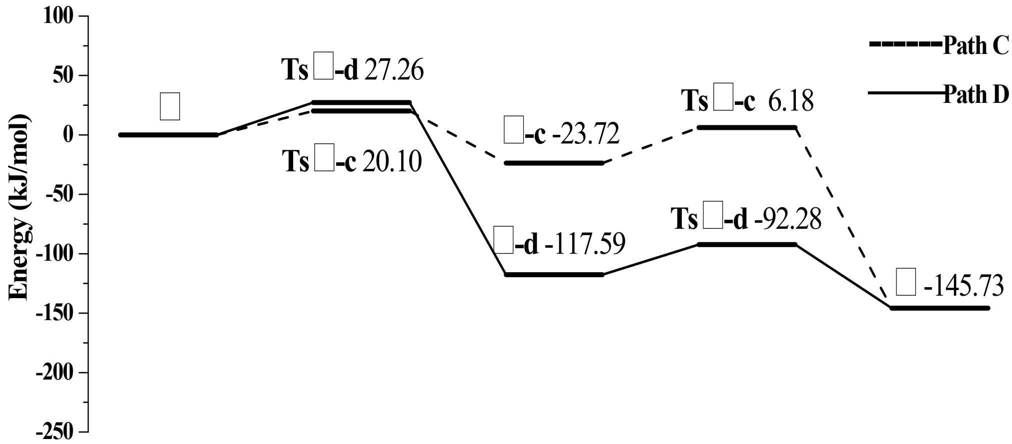

③	Ts ③-c	④-c	Ts ④-c
			
		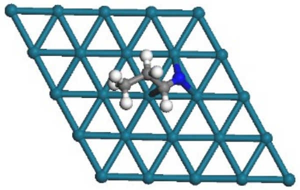	
Ts ③-d	**④-d**	**Ts ④-d**	⑤
			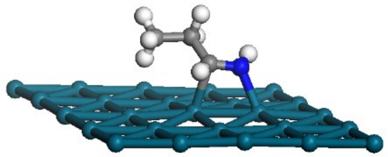
			

Fig.S13 Energy profile of propylene imine formation on Ni(111)

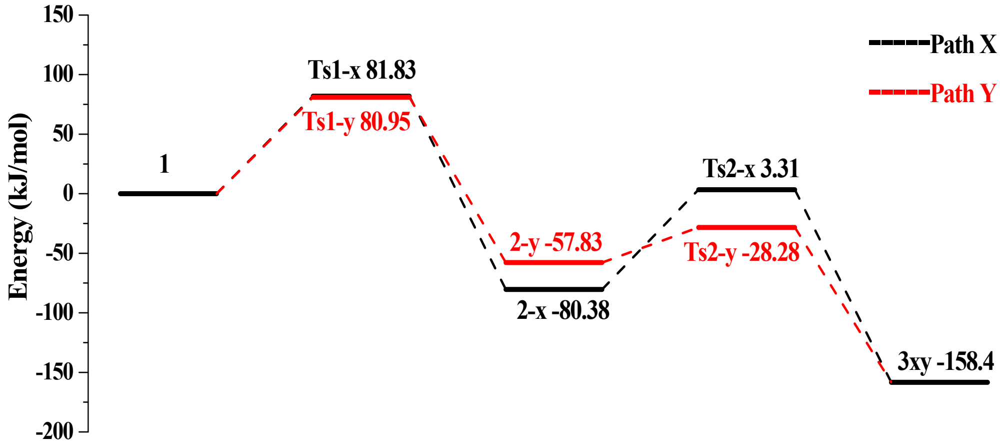

1	Ts1-x	2-x	Ts2-x
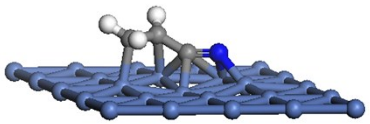	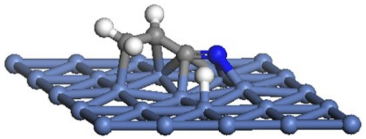	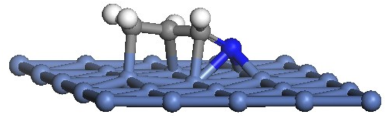	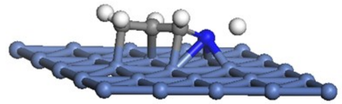
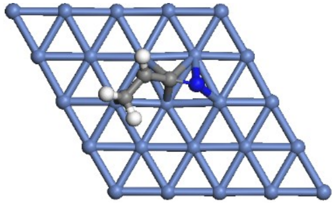	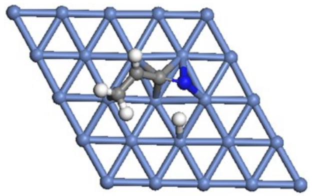	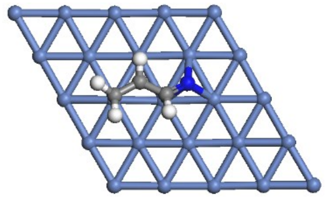	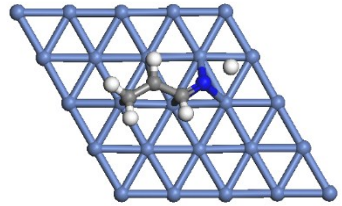
Ts1-y	**2-y**	**Ts2-y**	**3xy**
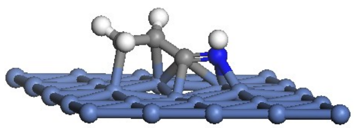	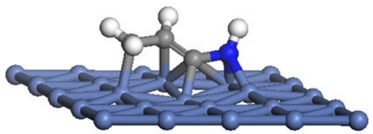	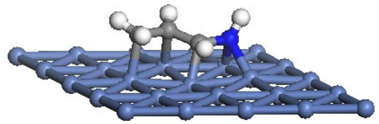	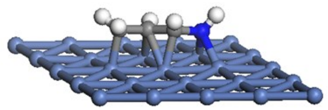
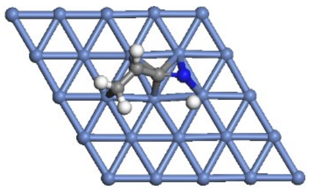	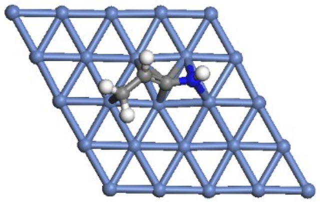	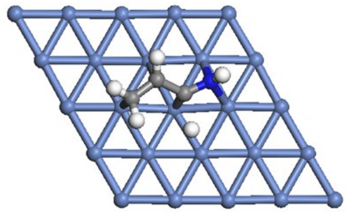	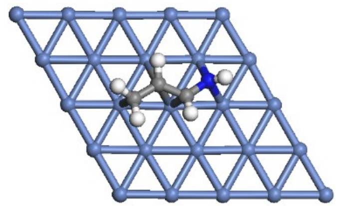

Fig.S14 Energy profile of propylene imine formation on Pd(111)

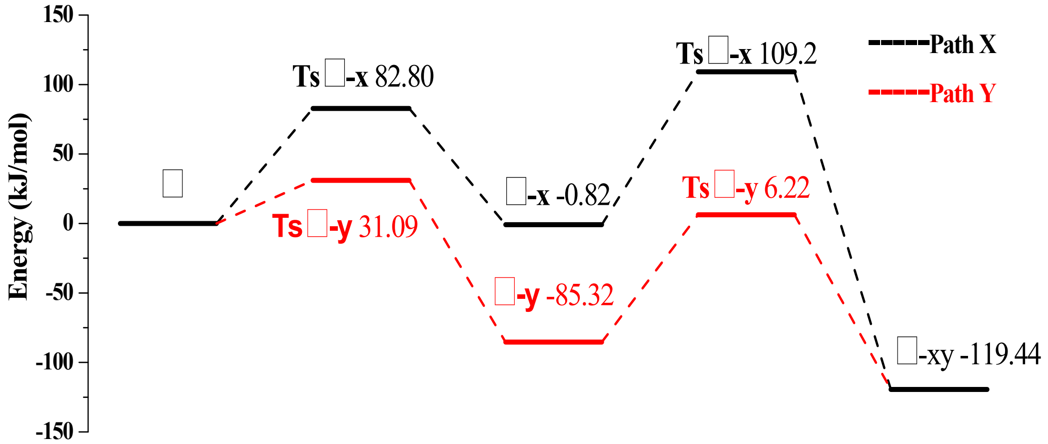

①	**Ts ①-x**	**②-x**	**Ts ②-x**
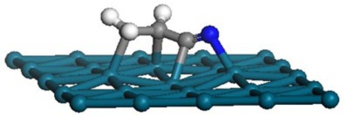	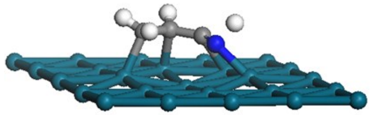	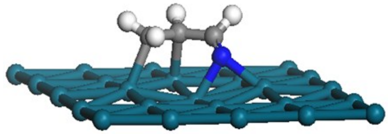	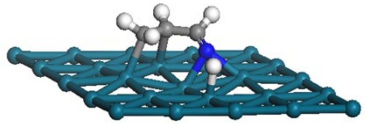
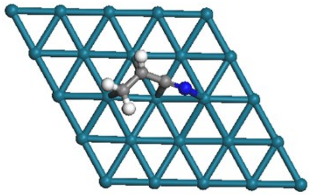	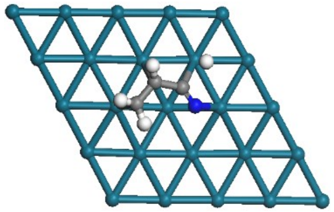	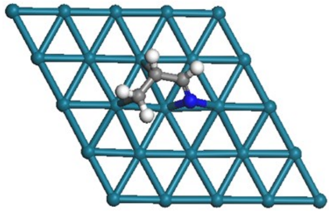	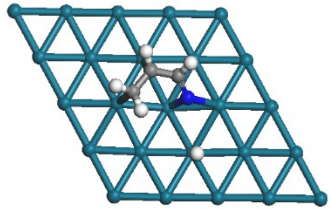
Ts ①-y	**②-y**	**Ts ②-y**	**③-xy**